Neuronal $Ca_V1.3\alpha_1$ L-Type Channels Activate at Relatively Hyperpolarized Membrane Potentials and Are Incompletely Inhibited by Dihydropyridines

Weifeng Xu and Diane Lipscombe

Department of Neuroscience, Brown University, Providence, Rhode Island 02912

L-type calcium channels regulate a diverse array of cellular functions within excitable cells. Of the four molecularly defined subclasses of L-type Ca channels, two are expressed ubiquitously in the mammalian nervous system ($Ca_V1.2\alpha_1$ and $Ca_V1.3\alpha_1$). Despite diversity at the molecular level, neuronal L-type channels are generally assumed to be functionally and pharmacologically similar, i.e., high-voltage activated and highly sensitive to dihydropyridines. We now show that $Ca_V1.3\alpha_1$ L-type channels activate at membrane potentials ~25 mV more hyperpolarized, compared with $Ca_V1.2\alpha_1$. This unusually negative activation threshold for $Ca_V1.3\alpha_1$ channels is independent of the specific auxiliary subunits coexpressed, of alternative splicing in domains I–II, IVS3–IVS4, and the C terminus, and of the expression system. The use of high concentrations of extracellular divalent cations has possibly obscured the unique voltage-dependent properties of $Ca_V1.3\alpha_1$ in certain previous studies. We also demonstrate that $Ca_V1.3\alpha_1$ channels are pharmacologically distinct from $Ca_V1.2\alpha_1$. The IC_{50} for nimodipine block of $Ca_V1.3\alpha_1$ L-type calcium channel currents is 2.7 ± 0.3 μM, a value 20-fold higher than the concentration required to block $Ca_V1.2\alpha_1$. The relatively low sensitivity of the $Ca_V1.3\alpha_1$ subunit to inhibition by dihydropyridine is unaffected by alternative splicing in the IVS3–IVS4 linker. Our results suggest that functional and pharmacological criteria used commonly to distinguish among different Ca currents greatly underestimate the biological importance of L-type channels in cells expressing $Ca_V1.3\alpha_1$.

Key words: $Ca_V1.3\alpha_1$; L-type; voltage-gated calcium channel; dihydropyridine; low threshold; R-type; clone; Xenopus *oocytes; HEK 293*

L-type calcium channels couple excitation to contraction in muscle, to gene expression in neurons, to hormone secretion in endocrine cells, and to transmitter release in hair cells (Beam et al., 1989; Ashcroft et al., 1994; Fuchs, 1996; Finkbeiner and Greenberg, 1998). Four genes encode L-type $Ca_V1\alpha_1$ subunits in mammals (Ertel et al., 2000). $Ca_V1.2\alpha_1$ (α_{1C}) and $Ca_V1.3\alpha_1$ (α_{1D}) are the two most widely expressed L-type channel subunits, and together they are thought to underlie L-type currents in neurons (Hell et al., 1993). Despite reports of functional diversity among L-type currents in select cells, notably endocrine cells, hippocampal neurons, and hair cells (Smith et al., 1993; Avery and Johnston, 1996; Kavalali and Plummer, 1996; Platzer et al., 2000), L-type channels are often assumed to be high voltage-activated and dihydropyridine-sensitive (Ertel et al., 2000). These defining criteria are used to establish the involvement of L-type channel in Ca signaling in a variety of cell types, including neurons. Functional studies of recombinant $Ca_V1.2\alpha_1$ subunits have confirmed that they form prototypic, high voltage-activated, long-lasting, dihydropyridine-sensitive L-type currents (Mori et al., 1993). However, comparable studies of $Ca_V1.3\alpha_1$ are limited (Williams et al., 1992; Ihara et al., 1995; Bell et al., 2001). We report that $Ca_V1.2\alpha_1$ and $Ca_V1.3\alpha_1$ L-type channels are significantly different both at the functional and pharmacological level, contrary to current classification schemes (Ertel et al., 2000). Our results suggest that functional and pharmacological criteria currently used to establish the relative contributions of different Ca channels to various signaling pathways will greatly underestimate the biological importance of L channels in cells that express $Ca_V1.3\alpha_1$. Their unique voltage dependence of activation also implies that $Ca_V1.3\alpha_1$ L-type Ca channels mediate cellular processes that depend on calcium influx at relatively hyperpolarized membrane potentials (Liljelund et al., 2000).

Received April 16, 2001; revised May 25, 2001; accepted May 31, 2001.

This work was supported by National Institutes of Health Grants NS29967 and NS01927. We thank Dr. Yasuo Mori for providing $Ca_V1.2\alpha_1$ cDNA, Drs. Kevin Campbell and Derrick Witcher for $Ca_V\beta_{1b}$ cDNA, and Dr. Edward Perez-Reyes for $Ca_V\beta_{2a}$ and $Ca_V\beta_4$ cDNAs. We thank Christopher Thaler and Annette Gray for their helpful comments on this manuscript.

Correspondence should be addressed to Diane Lipscombe, Department of Neuroscience, Brown University, 192 Thayer Street, Providence, RI 02912. E-mail: Diane_Lipscombe@brown.edu.

MATERIALS AND METHODS

Cloning. Full-length $Ca_V1.3\alpha_1$ cDNAs were constructed from overlapping rat superior cervical ganglia library- and RT-PCR-derived cDNAs. Library screening and RT-PCR methods have been described previously (Lin et al., 1997). The Expand High Fidelity PCR system (Roche Molecular Biochemicals, Indianapolis, IN) was used for PCR amplification. Library-derived cDNA clones, pRD9901, pRD9902, pRD9904 and pRD9905 were in pBluescript SK vector (Stratagene, La Jolla, CA). pRD9906 and pRD9907 were in pGEM-T vector (Promega, Austin, TX), derived from RT-PCR with primer pairs RDU2715 (5′-ACT TCA TCA TCC TTT TCA TCT GTG G-3′) and RDD3955 (5′-TGA CGA AGC CCA CGA AGA TAT TC-3′), and RDU6165 (5′-CTC TCC CAT TGG CTA TGA CTC AC-3′) and RDD6945 (5′-GCT ACA AGG TGG TGA TGC AAA TC-3′), respectively. The $(ATG)_7$ repeat in the 5′-untranslated region (UTR) was removed by PCR from a library-derived clone, RD9901, with primers RDU2 (5′-ATA TCG ATG CTA GCT GTT CGT GGA AAT GCA GCA TCA T-3′) and RDD711 (5′-AAT CCA GTA AGT TCC ATC CGT TCC-3′), leaving one ATG as the single translation initiation site. *Cla*I and *Nhe*I sites were introduced in the 5′-UTR to facilitate further cloning work. Standard cloning methods were used to generate four full-length $Ca_V1.3\alpha_1$ cDNA clones containing different combinations of three alternative splice sites (+/Δ exon 11, +/Δ exon 32, and exon 42a/exon 42). Exons are numbered according to the method of Yamada et al. (1995), except for exon 42a, which was present

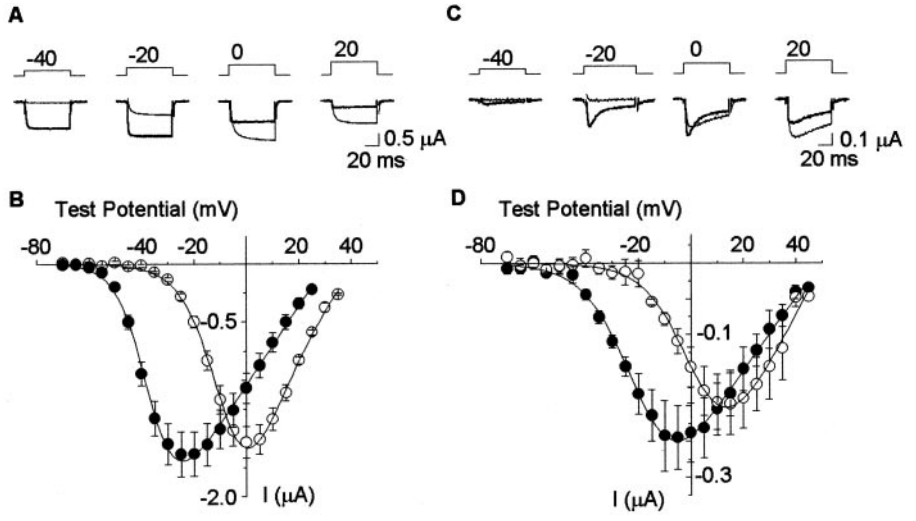

Figure 1. Two classes of L-type Ca channel activate at different voltages. *A*, Individual current traces measured from *Xenopus* oocytes transiently expressing $Ca_v1.3\alpha_1$ (*thick traces*) and $Ca_v1.2\alpha_1$ (*thin traces*), together with $Ca_V\beta_{1b}$, using 5 mM barium as the charge carrier. Currents were activated in response to voltage steps as indicated from a holding potential of −80 mV. *B*, Averaged, peak current–voltage plots for $Ca_v1.3\alpha_1$ (●) and $Ca_v1.2\alpha_1$ (○) channels using 5 mM barium as charge carrier. *C, D*, same as in *A* and *B*, except recordings were obtained using 5 mM calcium as the charge carrier. $V_{1/2}$ from peak current–voltage plot: with 5 mM barium as the charge carrier, $Ca_v1.3\alpha_1$ and $Ca_V\beta_{1b}$, −36.8 ± 0.8 mV ($n = 6$); $Ca_v1.2\alpha_1$ and $Ca_V\beta_{1b}$, −8.8 ± 0.8 mV ($n = 6$); with 5 mM calcium as the charge carrier, −20.0 ± 2.2 mV ($n = 4$) and 3.3 ± 2.0 mV ($n = 4$), respectively. Values are mean ± SE.

in one of our $Ca_V1.3\alpha_1$ cDNA clones and in the human genomic clone AC012467 that localizes to the $Ca_V1.3\alpha_1$ gene (3p14.3). The cDNAs were cloned into either pcDNA6 (Invitrogen, Carlsbad, CA) or into pBluescript (Stratagene) for expression. Unless indicated otherwise, the $Ca_V1.3\alpha_1$ variant used in these studies has the following combination of alternatively spliced exons: +exon11, Δexon32, and +exon42a (GenBank accession number AF370009).

Other clones. $Ca_V1.2\alpha_1$ cDNA was provided by Dr. Y. Mori (National Institute for Physiological Science, Okazaki, Japan; Mikami et al., 1989); $Ca_V\beta_{1b}$ cDNA was provided by Dr. K. P. Campbell (University of Iowa, Iowa City, IA; Pragnell et al., 1991); $Ca_V\beta_{2a}$ and $Ca_V\beta_4$ cDNAs were provided by Dr. E. Perez-Reyes (Loyola University, Marywood, IL; Castellano and Perez-Reyes, 1994), and $Ca_V\beta_3$ and $Ca_V\alpha_2\delta$ were cloned in our laboratory. The cDNAs were inserted in either pcDNA3 (Invitrogen) or pBluescript (Stratagene).

Transient expression and recording from Xenopus *oocytes.* Calcium channels were transiently expressed in *Xenopus* oocytes, and a two-microelectrode voltage clamp was used for recordings, essentially as described previously (Lin et al., 1999). Thirty nanograms of $Ca_V1.3\alpha_1$ or $Ca_V1.2\alpha_1$ together with 15 ng of $Ca_V\beta$ cRNA were injected into defolliculated *Xenopus* oocytes in a volume of 46 nl. Currents were recorded from oocytes 7–9 d after RNA injection. Fifteen to 30 min before recording, oocytes were injected with 46 nl of a 50 mM 1,2-bis(*o*-aminophenoxy)ethane-*N,N,N′,N′*-tetraacetate (BAPTA) solution to reduce activation of the endogenous calcium-activated chloride current (Lin et al., 1997). The estimated concentration of BAPTA inside the oocyte is 4.5 mM, assuming uniform dispersion from the point of injection and based on a cell radius of 0.5 mm. L-type calcium channel currents were recorded using 3 M KCl-filled electrodes with 0.7–1 and 0.4–0.7 MΩ resistances for voltage and current electrodes, respectively. The standard recording solution contained (in mM): 5 $BaCl_2$, 85 tetraethylammonium hydroxide (TEAOH), 5 KCl, and 5 HEPES, adjusted to pH 7.4 with methanesulphonic acid. When 2 mM $BaCl_2$ or 5 mM $CaCl_2$ was substituted for 5 mM $BaCl_2$, other components of the recording solutions remained the same. When 10, 20, and 40 mM $BaCl_2$ were used, tetraethylammonium was reduced to 75, 55, and 42.5 mM, respectively. The use of 3 M KCl agar bridges for grounding reduced junction potentials arising from changes in extracellular divalent cation concentration to <2 mV; therefore, no correction was made. Data were leak-subtracted on-line using a P/4 protocol (pClamp V6.0; Axon Instruments). Voltage steps were applied every 12 sec from a holding potential of −80 mV unless indicated otherwise. Peak current–voltage plots were fit with the following combination of the Goldman–Hodgkin–Katz (GHK) and Boltzmann equation to estimate activation midpoints: $I = \{P_1 \times P_2^2 \times V_m \times (1 - \exp(-(V_m - V_{rev} \times P_2))/(1 - \exp(-(V_m \times P_2))))\}/(1 + \exp(-(V_m - V_{1/2})/k))$, where V_m is the membrane potential; V_{rev} is the reversal potential; $V_{1/2}$ is the activation midpoint; P_1 is the permeability of the ion × $[Ca^{2+}]_i \times RT$; P_2 is zF/RT (z, the valency of the ion; F, the Faraday constant; R, the gas constant; and T, the temperature in degrees Kelvin); and k is Boltzmann constant.

Transient transfection and recording from tsA-201 cells. tsA-201 cells (large T-antigen transformed HEK293 cells) were transfected with 2.7 μg of a mix of $Ca_V1.3\alpha_1$, $Ca_V\beta_3$, and $Ca_V\alpha_2\delta$ in a molar ratio of 1:1:1, together with 0.3 μg of enhanced green florescent protein cDNA in a 60 mm tissue culture dish with 3 ml of growth media. Cells were transfected with the various cDNAs when 80% confluent, using LipofectAMINE-PLUS (Life Technologies, Gaithersburg, MD). Cells were trypsinized 36 hr later and plated on poly-D-lysine-coated coverslips for recording. Growth media contained DMEM supplemented with 10% FBS, 5 U/ml penicillin, and 5 μg/ml streptomycin, and cells were cultured at 37°C in 5% CO_2.

$Ca_V1.3\alpha_1$ currents were recorded from the majority of fluorescing tsA-201 cells (~80%). Whole-cell voltage-clamp recording was performed with the Axopatch 200A (Axon Instruments). Recording patch pipettes were fire-polished to a resistance of 2–6 MΩ. Sylgard (Dow Corning, Midland, MI) was used to decrease the pipette capacitance. The internal solution contained (in mM): 135 CsCl, 4 $MgCl_2$, 4 ATP, 10 HEPES, 10 EGTA, and 1 EDTA, adjusted to pH 7.2 with TEAOH. The bath solution contained: 135 mM CholineCl, 1 mM $MgCl_2$, 5 mM $BaCl_2$ or 2 mM $CaCl_2$ and 10 mM HEPES, adjusted to pH 7.2 with TEAOH. Series resistance was compensated 80%, with a 10 μs lag time. A voltage error of 4 mV attributable to the liquid junction potential was corrected for. Signals were sampled at 20 kHz and low pass-filtered at 2 kHz. Data were leak-subtracted on-line using a P/4 protocol and analyzed using pClamp V7.0 (Axon Instruments).

Pharmacology. Bay K 8644 (mixed enantiomer), nimodipine (a gift from Bayer), and nitrendipine (Sigma, St. Louis, MO) were dissolved in polyethylene glycol 400 at a concentration of 10 mM. (Stock solutions were stored at 4°C in the dark for up to 1 month.). The extracellular solution was exchanged at a rate of 5–10 ml/min.

RESULTS

We constructed a full-length $Ca_V1.3\alpha_1$ cDNA clone derived from rat sympathetic neurons. Figure 1 compares current–voltage relationships of L-type Ca channel currents recorded in *Xenopus* oocytes expressing either $Ca_V1.3\alpha_1$ or $Ca_V1.2\alpha_1$ together with the Ca channel $Ca_V\beta_{1b}$ subunit (5 mM barium as charge carrier). $Ca_V1.3\alpha_1$ and $Ca_V1.2\alpha_1$ currents show little or no inactivation during a 60 msec depolarizing pulse, a property typical of L-type currents recorded with barium as the charge carrier (Fig. 1*A*). Maximum currents in oocytes expressing $Ca_V1.2\alpha_1$ and $Ca_V1.3\alpha_1$ subunits were comparable in amplitude (−1.5 ± 0.1 μA, $n = 6$; and −1.6 ± 0.2 μA, $n = 6$, respectively). However, $Ca_V1.3\alpha_1$ currents activate at voltages significantly more negative compared with $Ca_V1.2\alpha_1$. With 5 mM barium as charge carrier, $Ca_V1.2\alpha_1$ generates prototypic, high voltage-activated L-type Ca channel currents that begin to activate at approximately −35 mV and peak at ~0 mV. In contrast, $Ca_V1.3\alpha_1$ currents activate at approximately −55 mV and reach ~60% of peak current at −40 mV, the very foot of the $Ca_V1.2\alpha_1$ current–voltage plot (Fig. 1*B*).

The large difference in the voltage dependence of activation between $Ca_V1.2\alpha_1$ and $Ca_V1.3\alpha_1$ currents was also observed with 5 mM calcium as the charge carrier (Fig. 1*C, D*). Interestingly, $Ca_V1.3\alpha_1$ currents showed more pronounced calcium-dependent inactivation compared with $Ca_V1.2\alpha_1$ (Fig. 1*C*).

There are reports that native L-type Ca currents in select cells can activate at relatively hyperpolarized membrane potentials (Smith et al., 1993; Avery and Johnston, 1996; Kavalali and Plummer, 1996; Platzer et al., 2000), but this is not a feature generally associated with L-type Ca channels (Ertel et al., 2000). Perhaps more perplexing, earlier studies of cloned $Ca_V1.3\alpha_1$ subunits derived from other tissues did not identify this channel as unique with regard to its voltage dependence of activation (Williams et al., 1992; Ihara et al., 1995; Bell et al., 2001).

A conspicuous difference in our studies of cloned $Ca_V1.3\alpha_1$ channels compared with others is the use of relatively low concentrations of divalent cations (5–10-fold lower than those typically used previously, 20 and 40 mM barium; Williams et al., 1992; Ihara et al., 1995; Bell et al., 2001). Voltage-gated ion channels, including Ca channels, are strongly influenced by the extracellular concentration of divalent cations as a result of surface charge screening effects (Frankenhaeuser and Hodgkin, 1957; Kostyuk et al., 1982). This led us to test whether higher divalent cation concentrations might obscure the negative activation threshold of $Ca_V1.3\alpha_1$ channels.

Figure 2 demonstrates that an increase in the extracellular concentration of barium from 2 to 40 mM increases the peak current approximately threefold, but more significantly, the voltage dependence of channel activation shifts toward more depolarized membrane potentials (~25 mV). Depolarizations to −40 mV evoke sizeable $Ca_v1.3\alpha_1$ currents with 2 mM extracellular barium, whereas the same depolarization barely activates the channels in 40 mM barium (Fig. 2*A*). A comparison of averaged, normalized peak current–voltage plots reveals an incremental shift in the voltage dependence of $Ca_v1.3\alpha_1$ channel activation with increasing concentrations of barium. These data suggest that $Ca_V1.3\alpha_1$ L-type Ca channels appear to be high-voltage activating when high concentrations of extracellular divalent cations are used.

The data presented in Figure 2 offer one explanation to account for differences between our findings and those reported previously. However, functional diversity exists among Ca channels containing the same $Ca_V\alpha_1$ subunit because of the potential to associate with different auxiliary subunits and because each $Ca_V\alpha_1$ gene is subject to extensive alternative splicing. Either of these factors at least has the potential to influence the voltage range over which $Ca_V1.3\alpha_1$ L-type Ca channels activate.

At least four different $Ca_v\beta$ subunits are expressed in mammals. Each $Ca_v\beta$ subunit can associate with multiple $Ca_v\alpha_1$ subunits, including L-type $Ca_v1\alpha_1$ subunits, *in vitro* and *in vivo* (Pichler et al., 1997; Walker and De Waard, 1998). $Ca_v\beta$ subunits have been shown to differentially modulate channel properties (Walker and De Waard, 1998). Therefore, we analyzed four $Ca_v1.3\alpha_1/Ca_v\beta$ subunit combinations. All four $Ca_v\beta$ subunits facilitated Ca channel current amplitudes compared with $Ca_v1.3\alpha_1$ alone (see legend to Fig. 3*A*), consistent with studies of other $Ca_v\alpha_1$ subunits (Walker and De Waard, 1998). A comparison of normalized current–voltage plots show that all four $Ca_v1.3\alpha_1$–$Ca_v\beta$ subunit combinations activate at membrane potentials that are at least 20 mV more hyperpolarized than $Ca_V1.2\alpha_1$ (Fig. 3*A*). We conclude that the association of $Ca_v1.3\alpha_1$ with any one of four different $Ca_v\beta$ subunits does not account for the large difference in channel activation thresholds that exists between $Ca_v1.2\alpha_1$ and $Cav1.3\alpha_1$.

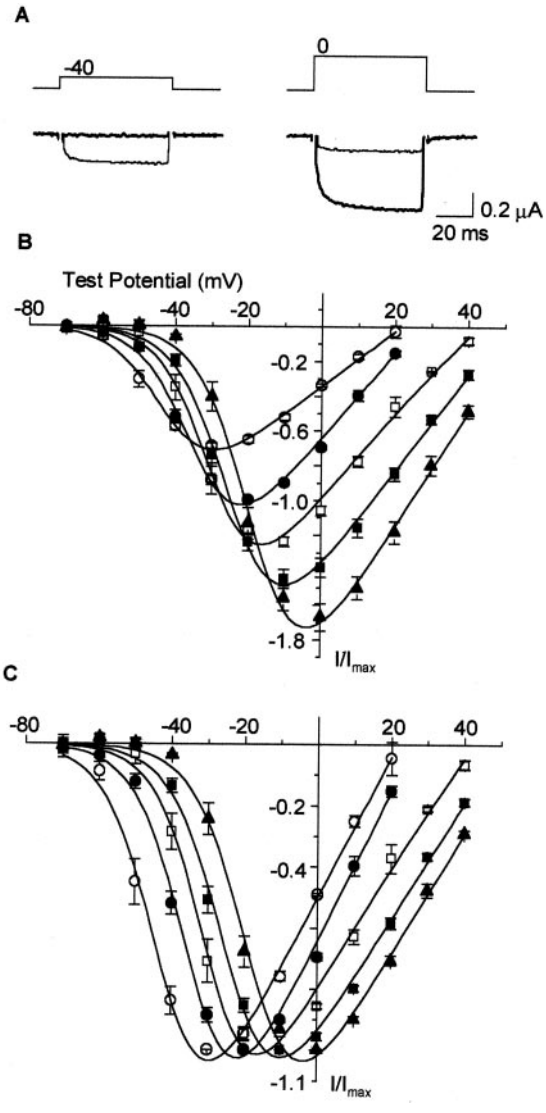

Figure 2. An increase in extracellular divalent cation concentration shifts the voltage dependence of $Ca_V1.3\alpha_1$ activation to depolarized potentials. *A*, Individual current traces measured from *Xenopus* oocytes transiently expressing $Ca_V1.3\alpha_1$ together with $Ca_V\beta_{1b}$, using 2 mM barium (*thin trace*) or 40 mM barium (*thick trace*) as the charge carrier. *B, C*, $Ca_V1.3\alpha_1$ channel currents recorded with 2 mM barium (○), 5 mM barium (●), 10 mM barium (□), 20 mM barium (■), and 40 mM barium (▲). Values plotted are averaged peak currents measured from each cell normalized to the maximum peak currents recorded with 5 mM barium (*B*) and averaged peak currents normalized to maximum peak current recorded at each barium concentration (*C*). $V_{1/2}$ from peak current–voltage plots: 2 mM barium, −42.7 ± 1.6 mV (n = 5); 5 mM barium, −33.8 ± 0.8 mV (n = 5); 10 mM barium, −29.6 ± 1.8 mV (n = 5); 20 mM barium, −24.7 ± 1.2 mV (n = 4); and 40 mM barium, −18.9 ± 1.6 mV (n = 4).

$Ca_V\alpha_2\delta$, another auxiliary subunit that associates with $Ca_v\alpha_1$, has the potential to modulate the voltage dependence of channel activation (Wakamori et al., 1999; Platano et al., 2000). We therefore compared peak current–voltage relationships of Ca channels recorded from oocytes expressing $Ca_v1.3\alpha_1$ and $Ca_v\beta_{1b}$ in the absence and presence of $Ca_V\alpha_2\delta$. The presence of the $Ca_V\alpha_2\delta$ subunit did not influence the voltage dependence of $Ca_v1.3\alpha_1$ current activation ($V_{1/2}$: $Ca_v1.3\alpha_1$ and $Ca_v\beta_{1b}$, −35.3 ±

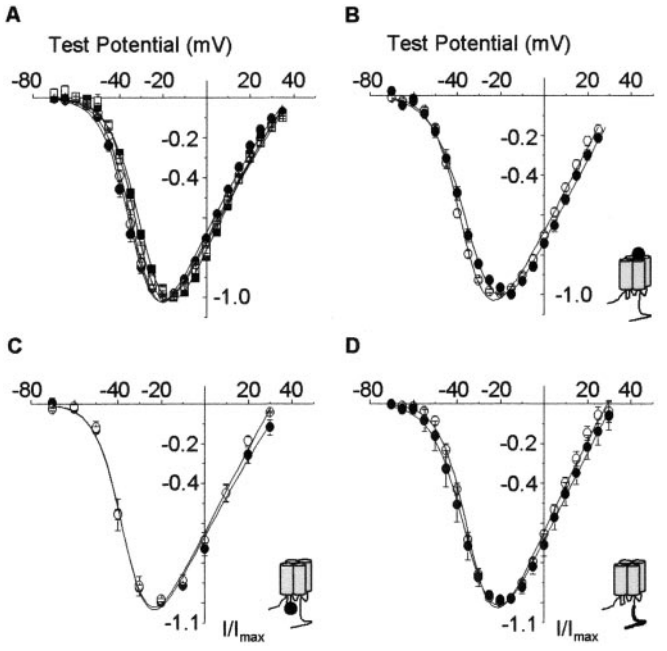

Figure 3. $Ca_V1.3\alpha_1$ channels open at relatively hyperpolarized voltages independent of several factors that potentially affect the voltage dependence of activation. Shown are comparisons of normalized, averaged peak current–voltage plots of $Ca_V1.3\alpha_1$ coexpressed with $Ca_V\beta_{1b}$ (●), $Ca_V\beta_{2a}$ (○), $Ca_V\beta_3$ (■), or $Ca_V\beta_4$ (□) subunits (*A*); with (●) or without (○) exon 32, which encodes a 15-amino acid sequence, PSDSENIPLPTATPG, in domain IVS3–IVS4 coexpressed with $Ca_V\beta_{1b}$ (*B*); with (●) or without (○) exon 11, which encodes a 20-amino acid sequence, CWWKRRGAAKTGPSGCRRWG, in loop I–II coexpressed with $Ca_V\beta_{1b}$ (*C*); and with exon 42 (●) or exon 42a (○) coexpressed with $Ca_V\beta_{1b}$ (*D*), Ca channel currents were recorded with 5 mM barium as the charge carrier. Maximum, peak current amplitudes induced by coexpressing $Ca_v1.3\alpha_1$ with different $Ca_V\beta$ subunits were -1.3 ± 0.1 μA ($n = 7$; $Ca_V\beta_{1b}$), -2.8 ± 0.2 μA ($n = 8$; $Ca_V\beta_{2a}$), -1.0 ± 0.1 μA ($n = 7$; $Ca_V\beta_3$), and -1.0 ± 0.5 μA ($n = 4$; $Ca_V\beta_4$). $Ca_v1.3\alpha_1$ alone induced currents with amplitudes of -0.43 ± 0.05 μA ($n = 6$). Average $V_{1/2}$ values were: *A*, -33.0 ± 1.0 mV ($n = 7$; $Ca_V\beta_{1b}$), -32.1 ± 0.8 mV ($n = 8$; $Ca_V\beta_{2a}$), -28.4 ± 0.5 mV ($n = 7$; $Ca_V\beta_3$), and -30.0 ± 1.0 mV ($n = 4$; $Ca_V\beta_4$); *B*, -35.7 ± 0.5 mV ($n = 8$; Δexon 32) and -31.7 ± 0.7 mV ($n = 5$; +exon 32); *C*, -36.1 ± 1.6 mV ($n = 8$; Δexon 11) and -35.3 ± 0.6 mV ($n = 5$; +exon 11); and *D*, -33.9 ± 1.5 mV ($n = 3$; +exon42) and -32.9 ± 0.4 mV ($n = 5$; +exon 42a). Values are mean ± SE.

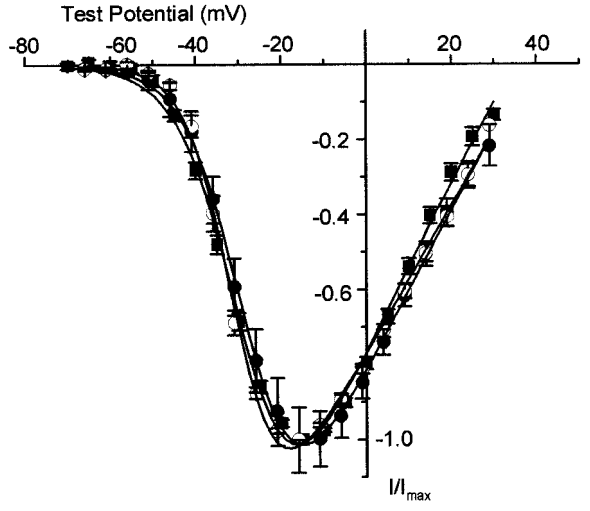

Figure 4. $Ca_V1.3\alpha_1$ channels open at relatively hyperpolarized voltages independent of expression system. Shown are normalized, averaged peak-$Ca_V1.3\alpha_1$ channel current–voltage plots recorded from *Xenopus* oocytes expressing $Ca_V1.3\alpha_1$ and $Ca_V\beta_3$ (5 mM Ba, ■) and tsA-201 cells expressing $Ca_V1.3\alpha_1$, $Ca_V\beta_3$, and $Ca_V\alpha_2\delta$ (5 mM Ba, ●; and 2 mM Ca, ○). Maximum peak currents were -1.0 ± 0.1 μA ($n = 7$, ■), -1.2 ± 0.1 nA ($n = 3$, ●), and -3.3 ± 1.0 nA ($n = 4$, ○). Average $V_{1/2}$ values were -28.4 ± 0.5 mV ($n = 7$, ■), -26.8 ± 0.7 mV ($n = 3$, ●), and -31.0 ± 0.8 mV ($n = 4$; ○), respectively. Values are mean ± SE.

0.6 mV, $n = 6$; $Ca_v1.3\alpha_1$, $Ca_v\beta_{1b}$, and $Ca_V\alpha_2\delta$, -36.8 ± 1.2 mV, $n = 6$) (see Fig. 4).

Nascent $Ca_v\alpha_1$ subunit RNAs, including $Ca_v1.3\alpha_1$, are subject to extensive alternative splicing (Perez-Reyes et al., 1990; Hui et al., 1991; Williams et al., 1992; Ertel et al., 2000). Alternative splicing occurs throughout the coding region of $Ca_v\alpha_1$ subunit genes and in some cases has been shown to influence the voltage dependence of Ca channel activation (Lin et al., 1997). Although the extent of alternative splicing in $Ca_v1.3\alpha_1$ has yet to be determined, we have characterized three regions of the gene that contain exons whose expression is regulated in a tissue-specific manner (Xu and Lipscombe, 2000). Exon 32 encodes 15 amino acids within domain IVS3–IVS4, and exon 11 encodes 20 amino acids in the I–II intracellular loop. Both these exons are alternatively spliced. Exons 42 and 42a in the C terminus are expressed in a mutually exclusive manner. The presence of exon 42a predicts a $Ca_v1.3\alpha_1$ subunit containing C termini 500 amino acids shorter than exon 42-containing subunits (GenBank accession number AF370010). We constructed four splice variants of $Ca_v1.3\alpha_1$ that differ in the expression of each exon and compared their properties (Fig. 3*B–D*). The current–voltage relationships of all $Ca_v1.3\alpha_1$ splice variants were virtually indistinguishable, and all activated at voltages that were ~20 mV more hyperpolarized than that of $Ca_v1.2\alpha_1$.

Finally, we studied the properties of $Ca_v1.3\alpha_1$ channel currents transiently expressed in a mammalian kidney cell line together with $Ca_V\alpha_2\delta$ and $Ca_v\beta_3$ (5 mM barium as charge carrier). $Ca_v1.3\alpha_1$ L-type currents expressed in tsA-201 cells are indistinguishable from those recorded in *Xenopus* oocytes (Fig. 4). The current–voltage curve of $Ca_v1.3\alpha_1$ L-type channel currents transiently expressed in tsA-201 cells with 2 mM calcium as the charge carrier is also shown to indicate the probable activation threshold of this current in neurons. Note that the position of the $Ca_v1.3\alpha_1$ current–voltage curve with 2 mM calcium is comparable with that recorded in 5 mM barium (Fig. 4). This is consistent with previous studies showing that calcium is more effective at shifting the gating of voltage-gated ion channels compared with barium (Hille, 1992).

Figures 1–4 demonstrate that L-type Ca channels are not all high voltage-activated as often assumed. However, in addition to biophysical criteria, L-type Ca channels are also, and more often, defined by their high sensitivity to dihydropyridine agonists and antagonists (Bean, 1989; Ertel et al., 2000). We therefore studied the pharmacological sensitivity of $Ca_v1.3\alpha_1$ and $Ca_v1.2\alpha_1$ to dihydropyridines. Bay K 8644 augmented $Ca_v1.3\alpha_1$ L-type currents and induced an ~10 mV shift in the voltage dependence of activation toward more hyperpolarized voltages compared with control (Fig. 5). Bay K 8644 also slowed channel activation and deactivation kinetics, consistent with its effects on other $Ca_v\ 1\alpha_1$ L-type currents (Grabner et al., 1996). $Ca_v1.3\alpha_1$ L-type channel currents were also inhibited by the dihydropyridine antagonist nimodipine. The degree of nimodipine-induced inhibition of $Ca_v1.3\alpha_1$ channel currents, however, differed significantly compared with $Ca_v1.2\alpha_1$. At 1 μM, nimodipine inhibited ~90% of the $Ca_v1.2\alpha_1$ channel current at voltages between −20 and +40 mV,

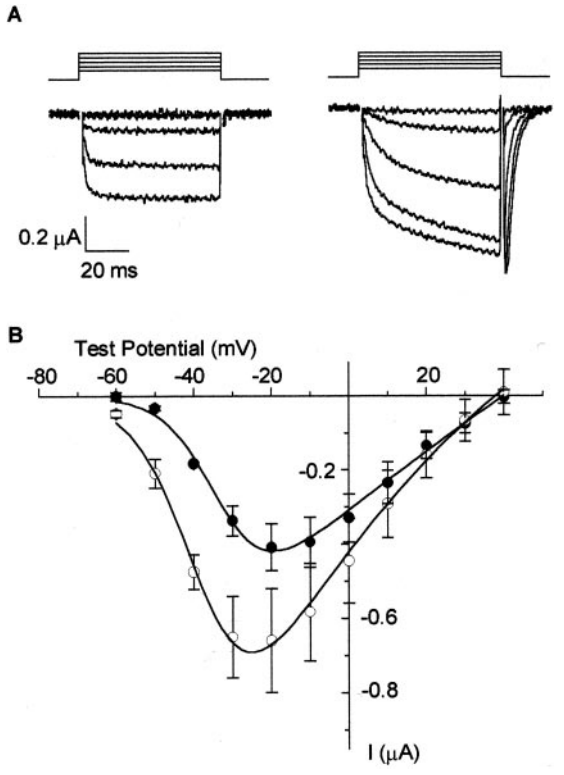

Figure 5. $Ca_V1.3\alpha_1$ currents were enhanced by Bay K 8644. *A*, $Ca_V1.3\alpha_1$ currents in the absence (*left*) and presence (*right*) of 1 μM Bay K 8644. Currents were activated from a holding potential of −80 mV. *B*, Averaged, peak current–voltage plots of $Ca_V1.3\alpha_1$ channels recorded with 5 mM barium in control (●) and in the presence of 1 μM Bay K 8644 (○). Maximum peak currents were −0.4 ± 0.1 μA (n = 3, ●) and −0.7 ± 0.1 μA (n = 3, ○). Average $V_{1/2}$ values were −32.2 ± 1.1 mV in control (n = 3, ●) and −39.0 ± 2.5 mV in the presence of Bay K 8644 (n = 3, ○).

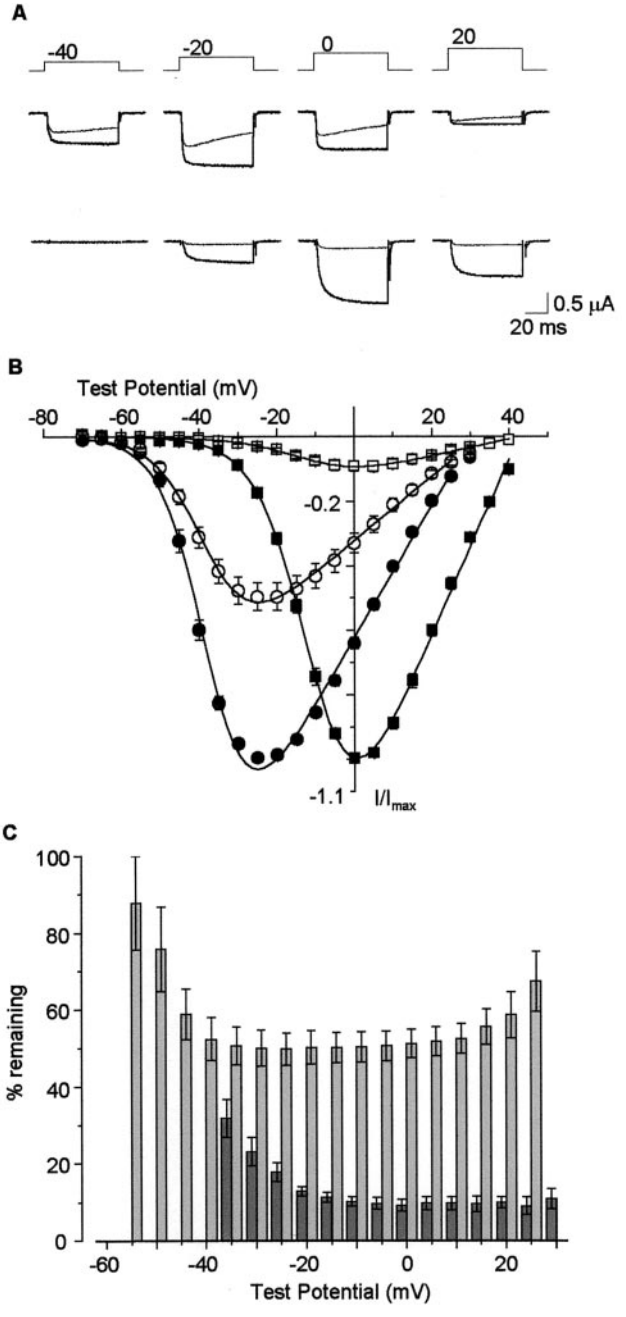

Figure 6. $Ca_V1.3\alpha_1$ currents are partially inhibited by dihydropyridines. *A*, $Ca_V1.3\alpha_1$ (*top*) and $Ca_V1.2\alpha_1$ (*bottom*) in the absence (*thick traces*) and presence (*thin traces*) of 1 μM nimodipine. Currents were activated by voltage steps as indicated, from a holding potential of −80 mV. *B*, Comparison of normalized, averaged peak current–voltage plots of $Ca_V1.3\alpha_1$ and $Ca_V1.2\alpha_1$ channels in the absence (●, ■) and presence (○, □) of 1 μM nimodipine, respectively. *C*, Peak $Ca_V1.3\alpha_1$ (*light gray*) and peak $Ca_V1.2\alpha_1$ (*dark gray*) currents remaining in the presence of nimodipine, plotted as percentage of control currents at various test potentials. Values are mean ± SE; n = 6 for $Ca_V1.3\alpha_1$ and n = 3 for $Ca_V1.2\alpha_1$.

whereas at the same concentration, peak $Ca_v1.3\alpha_1$ currents were inhibited ~50% at most (Fig. 6). Nimodipine was less effective at inhibiting both classes of L-type Ca channels at threshold voltages (Fig. 6*C*), consistent with a state-dependent blocking mechanism (Bean, 1984; Hess et al., 1984). Inhibition of peak $Ca_v1.2\alpha_1$ currents was, nonetheless, significantly greater compared with $Ca_v1.3\alpha_1$ at all membrane potentials (Fig. 6*B,C*). An examination of individual current traces shows that nimodipine induces an acceleration of the decay of the residual $Ca_v1.3\alpha_1$ current (Fig. 6*A*). However, even after a 60 msec depolarization, ~30% of the $Ca_v1.3\alpha_1$ current remained unblocked in the presence of 1 μM nimodipine. Figure 7*A* summarizes the pharmacological differences between $Ca_v1.3\alpha_1$ and $Ca_v1.2\alpha_1$ channels revealed by nimodipine. $Ca_V1.3\alpha_1$ channels are ~20-fold less sensitive to inhibition by nimodipine compared with $Ca_v1.2\alpha_1$ (Fig. 7*A*). Even at 10 μM, nimodipine did not completely inhibit the $Ca_v1.3\alpha_1$ current. The relatively low sensitivity of $Ca_v1.3\alpha_1$ to inhibition by dihydropyridine was confirmed using a second antagonist, nitrendipine (Fig. 7*B*). At 1 and 10 μM, nitrendipine reduced peak $Ca_v1.2\alpha_1$ currents by 64 ± 3% (n = 4) and 81 ± 1% (n = 4), respectively, but at these same concentrations only inhibited $Ca_v1.3\alpha_1$ currents by 23 ± 1% (n = 8) and 53 ± 2% (n = 8), respectively. The pharmacological sensitivity of $Ca_v1.3\alpha_1$ channels to dihydropyridine antagonists was unaffected by the presence or absence of exon 32 in the putative extracellular IVS3–IVS4 linker (Fig. 7*B*). Finally, we tested the effectiveness of the classic N-type Ca channel toxin ω-conotoxin GVIA to inhibit $Ca_v1.3\alpha_1$ channels. Others have reported that $Ca_v1.3\alpha_1$ channels are reversibly inhibited by high concentrations of this toxin (Williams et al., 1992). ω-Conotoxin GVIA did not inhibit $Ca_v1.3\alpha_1$ channel currents at concentrations up to 1 μM (99.0 ± 1.6%; n = 6, compared with control).

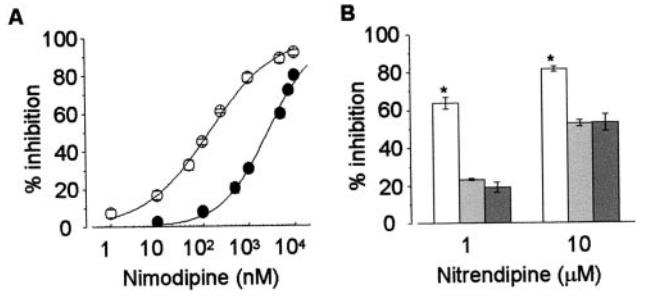

Figure 7. $Ca_V1.3\alpha_1$ and $Ca_V1.2\alpha_1$ channels are pharmacologically distinct. *A*, Dose–response curve of nimodipine inhibition of $Ca_V1.3\alpha_1$ (●) and $Ca_V1.2\alpha_1$ (○) channel currents. Data were fit to the Hill equation: $(I_{contol} - I_{nimodipine})/I_{control} = 1/(1 + (IC_{50}/C_{nimodipine})^h)$, where IC_{50} is the concentration of nimodipine required to inhibit 50% of peak current, and h is the Hill coefficient. $Ca_V1.3\alpha_1$, $IC_{50} = 2.7 \pm 0.3$ μM; $h = 0.85 \pm 0.04$ ($n = 5$); $Ca_V1.2\alpha_1$, $IC_{50} = 139 \pm 12$ nM; $h = 0.63 \pm 0.05$ ($n = 5$). *B*, Inhibition of $Ca_V1.3\alpha_1$ (Δexon 32, *light gray*, $n = 8$; +exon 32, *dark gray*, $n = 6$) and $Ca_V1.2\alpha_1$ (*white*, $n = 4$) by nitrendipine are significantly different at concentrations of 1 and 10 μM. Values are mean ± SE.

DISCUSSION

$Ca_v1.3\alpha_1$ L-channels open at relatively hyperpolarized membrane potentials

Our results suggest that calcium channels that contain the $Ca_v1.3\alpha_1$ subunit are not typical high voltage-activated L-type channels, and our study highlights the large difference in activation thresholds (~25 mV) between the two major classes of L-type channels expressed in neurons. This difference appears to stem from intrinsic differences between $Ca_v1.2\alpha_1$ and $Ca_v1.3\alpha_1$ genes, because it is independent of auxiliary subunits, alternative splicing in at least three different domains of the protein, and expression system (Figs. 3, 4). Given the unusually hyperpolarized activation threshold of $Ca_v1.3\alpha_1$ channels observed in our studies, it is perhaps surprising that this unique property has not been highlighted in previous studies of other $Ca_v1.3\alpha_1$ clones (Williams et al., 1992; Ihara et al., 1995; Bell et al., 2001). Although we cannot exclude the possibility that specific variants of $Ca_v1.3\alpha_1$ derived from other tissues or cell lines differ from our clones with respect to activation thresholds, we suggest that the use of high concentrations of extracellular divalent cations in certain studies may have obscured the unusually hyperpolarized activation range of $Ca_v1.3\alpha_1$ channels. For example, if our data are compared with those of Williams et al. (1992) under similar recording conditions (40 mM barium; Fig. 2), the $Ca_v1.3\alpha_1$ L-type current–voltage relationships are comparable. With 40 mM barium, the $Ca_v1.3\alpha_1$ current–voltage relationship is shifted to ~20 mV more depolarized. $Ca_v1.3\alpha_1$ L-type currents expressed in HEK293 cells (Bell et al., 2001; 20 mM barium) and Chinese hamster ovary cells (Ihara et al., 1995; 40 mM barium), however, activate at membrane potentials more depolarized compared with our data and with that of Williams et al. (1992), even after considering the effect of surface charge screening. The reasons for these differences are not apparent, given that Bell et al. (2001) used the same clone as that of Williams et al. (1992), and our results suggest that different expression systems do not influence the voltage dependence of $Ca_v1.3\alpha_1$ L-type channel activation (Fig. 4).

Is there evidence that native L-type $Ca_v1.3\alpha_1$ currents activate at hyperpolarized membrane potentials? Our studies of cloned $Ca_v1.3\alpha_1$ channels suggest that they activate at membrane potentials significantly more hyperpolarized than any $Ca_v1\alpha_1$ or $Ca_v2\alpha_1$ channel described to date. $Ca_v1.3\alpha_1$-containing L-type channels begin to activate at approximately −55 mV in the presence of 5 mM barium or 2 mM calcium, not as hyperpolarized as members of the T-type family but significantly more hyperpolarized relative to Ca_v $2.3\alpha_1$-containing (α_{1E}) channels (Perez-Reyes et al., 1998). Consistent with our studies of cloned channels, certain cells that express high levels of $Ca_v1.3\alpha_1$, such as hair cells and endocrine cells, contain native L-type Ca channels that activate at membrane potentials close to −50 mV (Smith et al., 1993; Zidanic and Fuchs, 1995; Kollmar et al., 1997). Perhaps most significantly, there is a selective loss of a low threshold-activating component of the whole cell Ca current in inner hair cells in $Ca_v1.3\alpha_1$-deficient mice (Platzer et al., 2000).

Although complicated by the presence of multiple classes of Ca channels with overlapping properties, there is evidence for the presence of low threshold-activating L-type Ca channels in neurons. For example, a component of low threshold-activating Ca current in CA3 pyramidal neurons of the hippocampus is reduced by high concentrations of dihydropyridines (Avery and Johnston, 1996). Furthermore, L-type Ca currents are thought to underlie spontaneous calcium oscillations that drive intrinsic activity in immature Purkinje cells of the cerebellum (Liljelund et al., 2000). Ca channels that drive spontaneous electrical activity are thought typically to activate at hyperpolarized membrane potentials (Bean, 1989). There is also evidence for the presence of two functionally distinct classes of L-type Ca channels from single-channel recordings in hippocampal neurons that differ significantly in their activation thresholds (Kavalali and Plummer, 1994, 1996). It would be interesting to test whether $Ca_v1.2\alpha_1$- and $Ca_v1.3\alpha_1$-containing channels underlie these different channels, because both these genes are expressed in the hippocampus (Hell et al., 1993). Our clone was isolated from sympathetic neurons, suggesting that a low-threshold L-type current exists in these cells. There is a low threshold-activating dihydropyridine- and conotoxin-resistant Ca current in sympathetic neurons that has been described in both whole-cell and single-channel recordings (Boland et al., 1994; Elmslie et al., 1994; Elmslie, 1997). It would be interesting to know whether at least part of the resistant current in sympathetic neurons originates from the activity of $Ca_v1.3\alpha_1$-containing channels (see below).

$Ca_v1.3\alpha_1$ calcium channels are less sensitive to dihydropyridine antagonists

High sensitivity to dihydropyridines is the universal indicator for the involvement of L-type calcium channels. However, at concentrations typically assumed to inhibit the majority of L-type Ca channels, ~50% of the peak $Ca_v1.3\alpha_1$ channel current remains unblocked in the presence of dihydropyridines (Figs. 6, 7). Support for the presence of native L-type channels in neurons that are incompletely inhibited by dihydropyridine antagonists is not simple to extract from available studies because of the prevalence of multiple classes of non-dihydropyridine-sensitive Ca channels in these cells. However, native L-type Ca currents in hair cells that express a relatively high density of $Ca_v1.3\alpha_1$ channels are incompletely inhibited by high concentrations of dihydropyridines (Zidanic and Fuchs, 1995; Platzer et al., 2000).

An additional feature of the dihydropyridine block of $Ca_v1.3\alpha_1$ channels is the altered inactivation kinetics of the residual Ca channel current. Although our study was not designed to address that mechanism, the dihydropyridine-induced inactivation profile is consistent with a state-dependent blocking model described for both native and cloned L-type Ca channels (Bean, 1984; Ber-

jukow et al., 2000). It is of interest, however, that high concentrations of dihydropyridines induce residual $Ca_v1.3\alpha_1$ L-type currents to inactivate during brief depolarizations, because similar low to mid threshold-activating and -inactivating and drug-resistant Ca channel currents have been described in a variety of neurons (Randall and Tsien, 1995; Avery and Johnston, 1996; Tottene et al., 1996). Such drug-resistant currents (or R-type currents) revealed by a mixture of Ca channel blockers that includes dihydropyridine antagonists have been attributed to the presence of non-L-type $Ca_v2.3\alpha_1$ (α_{1E}) subunits (Randall and Tsien, 1995; Tottene et al., 1996). $Ca_v2.3\alpha_1$ currents activate at somewhat hyperpolarized membrane potentials, inactivate with a relatively fast time course, and are resistant to various Ca channel blockers, including dihydropyridine antagonists (Ellinor et al., 1993; Randall and Tsien, 1995). However, the prevalence of significant drug-resistant Ca current in neurons of $Ca_v2.3\alpha_1$-deficient mice suggests that other $Ca_v\alpha_1$ subunits in addition to $Ca_v2.3\alpha_1$ contribute to this current (Wilson et al., 2000). On the basis of their similarities overall, it is likely that $Ca_v1.3\alpha_1$-containing channels underlie a significant fraction of the resistant Ca current described in neurons in the presence of Ca channel blockers.

Functional implications

L-type Ca channels have been implicated in regulating gene expression, cell survival, and synaptic plasticity in neurons (Galli et al., 1995; Norris et al., 1998; Mao et al., 1999; Weisskopf et al., 1999) and in supporting exocytosis in hair cells and pancreatic β cells (Ashcroft et al., 1994; Fuchs, 1996). However, our studies suggest that functional and pharmacological criteria currently used to distinguish among different Ca currents probably greatly underestimate the biological importance of L-type Ca channels in neurons expressing $Ca_v1.3\alpha_1$. The unique functional properties of $Ca_v1.3\alpha_1$ compared with $Ca_v1.2\alpha_1$ highlighted in the present study combine with evidence of distinct subcellular localization patterns (Hell et al., 1993) to imply that these two classes of L-type Ca channels may couple to different signaling pathways. Because of their unique properties, $Ca_v1.3\alpha_1$ channels are likely to be important for mediating Ca influx in response to relatively small membrane depolarizations, and our preliminary analysis of the voltage dependence of steady-state inactivation suggests that $Ca_v1.3\alpha_1$ L-type channels possess a significant window current at membrane potentials close to -50 mV. Such properties may be important for sustaining spontaneous rhythmic firing in neurons, traditionally attributed to the activity of low-threshold, T-type Ca channels (Bean, 1989; Ertel et al., 2000). Consistent with this, the dihydropyridine antagonist nimodipine partially suppresses spontaneous intracellular calcium oscillations and slows rhythmic firing in postnatal cerebellar Purkinje cells (Liljelund et al., 2000). More direct evidence for the involvement of $Ca_v1.3\alpha_1$ L-type Ca channels in driving rhythmic activity in excitable cells comes from studies of $Ca_v1.3\alpha_1$-deficient mice whose phenotype includes compromised sinoatrial node function (Platzer et al., 2000). A selective inhibitor of the $Ca_v1.3\alpha_1$ L-type current would greatly aid in establishing its contribution to the whole-cell Ca current in neurons and consequently its importance in coupling to downstream signaling pathways.

In summary, analysis of recombinant neuron-derived $Ca_v1.3\alpha_1$ channels has permitted functional and pharmacological characterization of this class of Ca current, which has been lacking. The unique properties of $Ca_v1.3\alpha_1$ contrast with the standard view of L-type Ca channels as high voltage-activated and highly sensitive to dihydropyridines and suggests that new functional roles for $Ca_v1.3\alpha_1$ L-type channels will be forthcoming.

Note added in proof. Properties similar to those described here were reported recently for a Ca_v $1.3\alpha_1$ subunit isolated from human pancreas (Koschak et al., 2001).

REFERENCES

Ashcroft FM, Proks P, Smith PA, Ammala C, Bokvist K, Rorsman P (1994) Stimulus-secretion coupling in pancreatic beta cells. J Cell Biochem 55:54–65.

Avery RB, Johnston D (1996) Multiple channel types contribute to the low-voltage-activated calcium current in hippocampal CA3 pyramidal neurons. J Neurosci 16:5567–5582.

Beam KG, Tanabe T, Numa S (1989) Structure, function, and regulation of the skeletal muscle dihydropyridine receptor. Ann NY Acad Sci 560:127–137.

Bean BP (1984) Nitrendipine block of cardiac calcium channels: high-affinity binding to the inactivated state. Proc Natl Acad Sci USA 81:6388–6392.

Bean BP (1989) Classes of calcium channels in vertebrate cells. Annu Rev Physiol 51:367–384.

Bell DC, Butcher AJ, Berrow NS, Page KM, Brust PF, Nesterova A, Stauderman KA, Seabrook GR, Nurnberg B, Dolphin AC (2001) Biophysical properties, pharmacology, and modulation of human, neuronal L-type (α_{1D}, $Ca_V1.3$) voltage-dependent calcium currents. J Neurophysiol 85:816–827.

Berjukow S, Marksteiner R, Gapp F, Sinnegger MJ, Hering S (2000) Molecular mechanism of calcium channel block by isradipine. Role of a drug-induced inactivated channel conformation. J Biol Chem 275:22114–22120.

Boland LM, Morrill JA, Bean BP (1994) ω-Conotoxin block of N-type calcium channels in frog and rat sympathetic neurons. J Neurosci 14:5011–5027.

Castellano A, Perez-Reyes E (1994) Molecular diversity of Ca^{2+} channel beta subunits. Biochem Soc Trans 22:483–488.

Ellinor PT, Zhang JF, Randall AD, Zhou M, Schwarz TL, Tsien RW, Horne WA (1993) Functional expression of a rapidly inactivating neuronal calcium channel. Nature 363:455–458.

Elmslie KS, Kammermeier PJ, Jone SW (1994) Reevaluation of Ca^{2+} channel types and their modulation in bullfrog sympathetic neurons. Neuron 13:17–28.

Elmslie KS (1997) Identification of the single channels that underlie the N-type and L-type calcium currents in bullfrog sympathetic neurons. J Neurosci 17:2658–2668.

Ertel EA, Campbell KP, Harpold MM, Hofmann F, Mori Y, Perez-Reyes E, Schwartz A, Snutch TP, Tanabe T, Birnbaumer L, Tsien RW, Catterall WA (2000) Nomenclature of voltage-gated calcium channels [letter, comment]. Neuron 25:533–535.

Finkbeiner S, Greenberg ME (1998) Ca^{2+} channel-regulated neuronal gene expression. J Neurobiol 37:171–189.

Frankenhaeuser B, Hodgkin AL (1957) The action of calcium on the electrical properties of squid axons. J Physiol (Lond) 137:218–244.

Fuchs PA (1996) Synaptic transmission at vertebrate hair cells. Curr Opin Neurobiol 6:514–519.

Galli C, Meucci O, Scorziello A, Werge TM, Calissano P, Schettini G (1995) Apoptosis in cerebellar granule cells is blocked by high KCl, forskolin, and IGF-1 through distinct mechanisms of action: the involvement of intracellular calcium and RNA synthesis. J Neurosci 15:1172–1179.

Grabner M, Wang Z, Hering S, Striessnig J, Glossmann H (1996) Transfer of 1,4-dihydropyridine sensitivity from L-type to class A (BI) calcium channels. Neuron 16:207–218.

Hell JW, Westenbroek RE, Warner C, Ahlijanian MK, Prystay W, Gilbert MM, Snutch TP, Catterall WA (1993) Identification and differential subcellular localization of the neuronal class C and class D L-type calcium channel alpha 1 subunits. J Cell Biol 123:949–962.

Hess P, Lansman JB, Tsien RW (1984) Different modes of Ca channel gating behaviour favoured by dihydropyridine Ca agonists and antagonists. Nature 311:538–544.

Hille B (1992) Ionic channels of excitable membranes. Sunderland, MA: Sinauer.

Hui A, Ellinor PT, Krizanova O, Wang JJ, Diebold RJ, Schwartz A (1991) Molecular cloning of multiple subtypes of a novel rat brain isoform of the alpha 1 subunit of the voltage-dependent calcium channel. Neuron 7:35–44.

Ihara Y, Yamada Y, Fujii Y, Gonoi T, Yano H, Yasuda K, Inagaki N, Seino Y, Seino S (1995) Molecular diversity and functional characterization of voltage-dependent calcium channels (CACN4) expressed in pancreatic beta-cells. Mol Endocrinol 9:121–130.

Kavalali ET, Plummer MR (1994) Selective potentiation of a novel calcium channel in rat hippocampal neurones. J Physiol (Lond) 480:475–484.

Kavalali ET, Plummer MR (1996) Multiple voltage-dependent mechanisms potentiate calcium channel activity in hippocampal neurons. J Neurosci 16:1072–1082.

Kollmar R, Montgomery LG, Fak J, Henry LJ, Hudspeth AJ (1997) Predominance of the alpha1D subunit in L-type voltage-gated Ca^{2+} channels of hair cells in the chicken's cochlea. Proc Natl Acad Sci USA 94:14883–14888.

Koschak A, Reimer D, Huber I, Grabner M, Glossmann H, Engel J, Striessnig J (2001) α1D (cav1.3) subunits can form L-type Ca^{2+} channels activating at negative voltages. J Biol Chem 276:22100–22106.

Kostyuk PG, Mironov SL, Doroshenko PA, Ponomarev VN (1982) Surface charges on the outer side of mollusc neuron membrane. J Membr Biol 70:171–179.

Liljelund P, Netzeband JG, Gruol DL (2000) L-Type calcium channels mediate calcium oscillations in early postnatal purkinje neurons. J Neurosci 20:7394–7403.

Lin Z, Haus S, Edgerton J, Lipscombe D (1997) Identification of functionally distinct isoforms of the N-type Ca^{2+} channel in rat sympathetic ganglia and brain. Neuron 18:153–166.

Lin Z, Lin Y, Schorge S, Pan JQ, Beierlein M, Lipscombe D (1999) Alternative splicing of a short cassette exon in α_{1B} generates functionally distinct N-type calcium channels in central and peripheral neurons. J Neurosci 19:5322–5331.

Mao Z, Bonni A, Xia F, Nadal-Vicens M, Greenberg ME (1999) Neuronal activity-dependent cell survival mediated by transcription factor MEF2. Science 286:785–790.

Mikami A, Imoto K, Tanabe T, Niidome T, Mori Y, Takeshima H, Narumiya S, Numa S (1989) Primary structure and functional expression of the cardiac dihydropyridine-sensitive calcium channel. Nature 340:230–233.

Mori Y, Niidome T, Fujita Y, Mynlieff M, Dirksen RT, Beam KG, Iwabe N, Miyata T, Furutama D, Furuichi T, Mikoshiba K (1993) Molecular diversity of voltage-dependent calcium channel. Ann NY Acad Sci 707:87–108.

Norris CM, Halpain S, Foster TC (1998) Reversal of age-related alternations in synaptic plasticity by blockade of L-type Ca^{2+} channels. J Neurosci 18:3171–3179.

Perez-Reyes E, Wei XY, Castellano A, Birnbaumer L (1990) Molecular diversity of L-type calcium channels. Evidence for alternative splicing of the transcripts of three non-allelic genes. J Biol Chem 265:20430–20436.

Perez-Reyes E, Cribbs LL, Daud A, Lacerda AE, Barclay J, Williamson MP, Fox M, Rees M, Lee JH (1998) Molecular characterization of a neuronal low-voltage-activated T-type calcium channel. Nature 391:896–900.

Pichler M, Cassidy TN, Reimer D, Haase H, Kraus R, Ostler D, Striessnig J (1997) Beta subunit heterogeneity in neuronal L-type Ca^{2+} channels. J Biol Chem 272:13877–13882.

Platano D, Qin N, Noceti F, Birnbaumer L, Stefani E, Olcese R (2000) Expression of the alpha(2)delta subunit interferes with prepulse facilitation in cardiac L-type calcium channels. Biophys J 78:2959–2972.

Platzer J, Engel J, Schrott-Fischer A, Stephan K, Bova S, Chen H, Zheng H, Striessnig J (2000) Congenital deafness and sinoatrial node dysfunction in mice lacking class D L-type Ca^{2+} channels. Cell 102:89–97.

Pragnell M, Sakamoto J, Jay SD, Campbell KP (1991) Cloning and tissue-specific expression of the brain calcium channel beta-subunit. FEBS Lett 291:253–258.

Randall A, Tsien RW (1995) Pharmacological dissection of multiple types of Ca^{2+} channel currents in rat cerebellar granule neurons. J Neurosci 15:2995–3012.

Smith PA, Ashcroft FM, Fewtrell CM (1993) Permeation and gating properties of the L-type calcium channel in mouse pancreatic beta cells. J Gen Physiol 101:767–797.

Tottene A, Moretti A, Pietrobon D (1996) Functional diversity of P-type and R-type calcium channels in rat cerebellar neurons. J Neurosci 16:6353–6363.

Wakamori M, Mikala G, Mori Y (1999) Auxiliary subunits operate as a molecular switch in determining gating behaviour of the unitary N-type Ca^{2+} channel current in *Xenopus* oocytes. J Physiol (Lond) 517:659–672.

Walker D, De Waard M (1998) Subunit interaction sites in voltage-dependent Ca^{2+} channels: role in channel function. Trends Neurosci 21:148–154.

Weisskopf MG, Bauer EP, LeDoux JE (1999) L-type voltage-gated calcium channels mediate NMDA-independent associative long-term potentiation at thalamic input synapses to the amygdala. J Neurosci 19:10512–10519.

Williams ME, Feldman DH, McCue AF, Brenner R, Velicelebi G, Ellis SB, Harpold MM (1992) Structure and functional expression of alpha 1, alpha 2, and beta subunits of a novel human neuronal calcium channel subtype. Neuron 8:71–84.

Wilson SM, Toth PT, Oh SB, Gillard SE, Volsen S, Ren D, Philipson LH, Lee EC, Fletcher CF, Tessarollo L, Copeland NG, Jenkins NA, Miller RJ (2000) The status of voltage-dependent calcium channels in alpha 1E knock-out mice. J Neurosci 20:8566–8571.

Xu W, Lipscombe D (2000) Splice variants of the L-type Ca channel α_{1D} subunit. Soc Neurosci Abstr 26:101.

Yamada Y, Masuda K, Li Q, Ihara Y, Kubota A, Miura T, Nakamura K, Fujii Y, Seino S, Seino Y (1995) The structures of the human calcium channel alpha 1 subunit (CACNL1A2) and beta subunit (CACNLB3) genes. Genomics 27:312–319.

Zidanic M, Fuchs PA (1995) Kinetic analysis of barium currents in chick cochlear hair cells. Biophys J 68:1323–1336.